Applied Acoustics 203 (2023) 109192

Contents lists available at ScienceDirect

Applied Acoustics

journal homepage: www.elsevier.com/locate/apacoust

Energy trapping in a phononic crystal cavity enhanced by nonreciprocal acoustic wave transmission

Jyotsna Dhillon [a], Ezekiel Walker [b], Arkadii Krokhin [a,*], Arup Neogi [c,*]

[a] Department of Physics, University of North Texas, P.O. Box 311427, Denton, TX 76203, USA
[b] Echonovus Inc, 1800 South Loop 288 STE 396 #234, Denton, TX 76205, USA
[c] Institute of Fundamental and Frontier Sciences, University of Electronic Science and Technology of China, Chengdu 611731, China

ARTICLE INFO

Article history:
Received 29 September 2022
Received in revised form 30 November 2022
Accepted 28 December 2022

ABSTRACT

Defect mode induced energy trapping at the bandgap frequency of a phononic crystal has been widely explored. Unlike this extensively used mechanism, this work reports the use of nonreciprocity in the transmission band to trap energy inside a phononic crystal cavity. Passive nonreciprocity is due to natural viscosity of the background liquid (water) and asymmetry of aluminum scatterers. The level of non-resonant energy trapping was compared for three cavities with different symmetry. Enhancement of energy trapping at a frequency of 624 kHz was observed experimentally for the cavity where nonreciprocity suppresses acoustic radiation into environment. Experimental results were further investigated and confirmed using finite element numerical analysis.

1. Introduction

Phononic crystal-based metamaterials exhibit reach dispersive and scattering properties allowing existence of band gaps [1–3], negative refraction [4,5], localization [6–9], resonant defect modes [10–12] and other nontrivial effects. The phononic crystals comprise arrays of elastic scatterers periodically arranged in a matrix maintaining high impedance mismatch with their surrounding medium. Similar to their well-studied photonic crystal analogs, wave propagation may be restricted in specific directions due to a partial bandgap, or all directions in a full bandgap. Bandgap characteristics in phononic crystals have been exploited in various acoustic applications, including but not limited to sound insulation, imaging, communication, acoustic cloaking, and sensors.

The removal or modification of lattice scatterers introduces lattice defects or cavities and gives rise to localized resonant modes. Extensive efforts have been devoted to exploring the effect of defects on resonance modes in various types of crystals, particularly as it applies to waveguides, filtering, and energy trapping [13–17]. The phenomenon of energy trapping using resonant modes has been explored for phononic crystals. The resonant frequency arises in the bandgap region and the acoustic energy associated with it gets confined within the cavity.

Confinement of acoustic waves inside crystalline defects using various forms has been reported. Khelif, et al. demonstrated confinement of a resonant mode inside a defect of a 2D phononic crystal where the resonant mode was within a complete bandgap [10]. Other reports include micromechanical resonators operating as Bragg mirrors for confinement [18] and acoustic energy harvesters for energy conversion [19]. These systems, being time-reversible, are all reciprocal, leveraging broken periodicity that gives rise to a discrete level within a bandgap.

Recently, nonreciprocity was explored for dissipative phononic crystals using asymmetric scatterers with results demonstrating the potential for energy trapping [20]. Nonreciprocity is generally defined by the breaking of time reversal symmetry of an elastic medium where a wave propagates. For a reciprocal medium, two stationary points serving as a source and detector will have indistinguishable pressure detection when interchanged as described by the Rayleigh reciprocity theorem [21]. Nonreciprocity violates this convention, with detection being distinguishable, dependent on which point serves as the source.

Various methods for generating nonreciprocal systems have been reported in acoustic and electromagnetic systems [22,23]. Though other methods utilize active or nonlinear media to achieve nonreciprocity, the present work utilizes the passive linear mechanism of loss-induced nonreciprocity as demonstrated in [20,24]. Furthermore, it is also concluded in [24] that the observed distinguishable detection in such system is due to the contribution of two factors, i.e., asymmetry of scatterers, which does not break the reciprocity of the system, and dissipation caused by the vorticity mode of oscillating fluid velocity with $\nabla \times \mathbf{v} \neq 0$, which exists only in a viscous medium. The vorticity mode reaches its

* Corresponding authors.
E-mail addresses: arkady@unt.edu (A. Krokhin), arup@uestc.edu.cn (A. Neogi).

https://doi.org/10.1016/j.apacoust.2022.109192
0003-682X/

maximum within a narrow boundary layer of thickness $\delta = \sqrt{2\eta/(\omega\rho)}$, where η is the viscous coefficient and ρ is the fluid density. Viscous losses break the time-reversal symmetry of the system making it irreversible in general and nonreciprocal if mirror symmetry (P symmetry) is broken by asymmetric scatterers. The passive, linear, and time-invariant mechanism of nonreciprocity presents a feasible opportunity to investigate energy trapping.

Dynamics of viscous fluid follow the Navier-Stokes equation for velocity $\mathbf{v}$. While the field of acoustic velocities in viscous fluid in the presence of scatterers differs essentially from that in ideal fluid, the scalar field of pressures $p(\mathbf{r})$ holds the same reciprocal symmetry $p_A(\mathbf{r}_B) = p_B(\mathbf{r}_A)$ between emitter and receiver upon switching their positions at points A and B. This property follows from the linearized continuity equation $-i\omega p + c^2\rho\nabla\cdot\mathbf{v} = 0$. The vorticity mode of velocity with $\nabla\times\mathbf{v}\neq 0$ does not contribute to this equation and pressure is defined by the potential part of velocity field. Since the Rayleigh reciprocity theorem [21] is valid for the potentials of velocity, pressure remains a reciprocal quantity even in a viscous fluid. Unlike this, the velocity itself does not possess the reciprocal symmetry even in inviscid fluid. The Linearized Euler equation for ideal fluid gives that $\mathbf{v} = \nabla p/i\omega\rho$. Even in a homogeneous ideal fluid where $\rho(\mathbf{r}) = const$, the reciprocal symmetry of pressure $p(\mathbf{r})$ is lost for ∇p if the scatterers the wave meets propagating from A to B are not symmetrical. This lack of symmetry for velocity field $\mathbf{v}_A(\mathbf{r}_B)\neq\mathbf{v}(\mathbf{r}_A)$ and acoustic intensity $I(\mathbf{r}) = v(\mathbf{r})p(\mathbf{r})$ does not mean nonreciprocity since dynamics of ideal fluid is time reversible, i.e., T symmetry is not broken.

In a viscous fluid propagation of sound becomes irreversible due to energy losses. Moreover, asymmetry in distribution of velocities for forward and backward propagation generates different viscous losses, which depend on the gradients of velocities $\partial v_i/\partial x_k$. These gradients are strongly influenced not only by the scatterer shape, but by scatterer surface features that interact with the viscous boundary layer. Thus, the asymmetry in distribution of intensities existing in ideal fluid acquires truly nonreciprocal contribution leading to different attenuation of forward ($A\rightarrow B$) and backward ($B\rightarrow A$) sound wave. The necessary condition for the viscosity-induced nonreciprocity to be manifested is broken mirror symmetry (or P symmetry) in the distribution of scatterers. Otherwise, propagation, being irreversible, remains reciprocal since dissipative losses are obviously equal for forward and backward propagation.

It is worth mentioning that in a viscous fluid the amplitude of sound tends exponentially to zero with distance between source and receiver. Therefore, propagation along an infinite path becomes reciprocal. In a dissipative phononic crystal the rates the amplitudes of Bloch waves with wave vector $\mathbf{k}$ and -$\mathbf{k}$ tends to zero becomes equal, independently of the symmetry of the scatterer and the unit cell [24]. Thus, the nonreciprocity caused by broken PT symmetry is a size effect which tends to zero for very long samples. In a dissipative phononic crystal with asymmetric scatterers viscous losses become directional-dependent [25] that makes it not only a nonreciprocal structure but also a metamaterial with anisotropic viscosity where in a wave propagating along different crystallographic directions loses different amount of its energy.

Energy trapping inside a phononic crystal cavity has not yet been explored using the transmission band of a nonreciprocal crystal. Here, we investigate and demonstrate the use of passive nonreciprocity to enhance energy trapping in a 2D phononic crystal. The scatterers are solid asymmetric circle sectors in water ambient as presented in Ref. [20]. A large cavity is introduced, the orientation of half the rods modified, and metrics concerning the average intensity inside and out the cavity closely examined both numerically and experimentally. Nonreciprocity is confirmed in the samples, used to increase the cavity intensity as compared with acoustically reciprocal samples, and the findings given below.

2. Methods

A 2D phononic crystal was fabricated with aluminum rods periodically arranged in a finite 14 × 9 rectangular lattice of lattice constant 5.5 mm (Fig. 1a) in water ambient (Fig. 1b). The aluminum scatterers are 120° asymmetric sections of a 2.2 mm radius cylinder (Fig. 1a). For investigation of trapped acoustic energy, a cavity was incorporated by removing a 4 × 5 section of scatterers from the crystal center, as depicted in Fig. 1b. Here, 0° (forward propagation) is defined as the wave incident on the curved surface of a scatterer, and 180° (reverse propagation) as incident on the cone (Fig. 1a).

Three types of cavities were fabricated and used in acoustic experiments, see Fig. 1c-d. All three cavities have identical incident halves consisting of 7 rows of rods (from left in Fig. 1b-d). In the latter half of the crystal, the rods are i) the same orientation (Fig. 1c), ii) reoriented by 180° (Fig. 1d), and iii) reoriented by 90° (Fig. 1e). Incident sound comes from the left at 0°. While all three cavities are of the same rectangular shape, they are of different symmetry. Symmetry is of principal importance for manifestation of the effect of nonreciprocity. The cavity in Fig. 1c is an extended defect in otherwise homogeneous crystal. It possesses the periodicity of the original phononic crystal. The cavity in Fig. 1d has extra mirror reflection symmetry about the central vertical line. This line is a twin boundary. The cavity in Fig. 1e is formed by two twin crystals rotated by 90°. The central vertical line is a cross-twin boundary with a cavity possessing the lowest symmetry. We will refer to these cavities as homogeneous (Fig. 1c), symmetric (Fig. 1d), and perpendicular (Fig. 1e).

The intensity of sound waves was measured inside and outside each cavity in a bistatic setup, as depicted in Fig. 1b. Incident ultrasound was generated from an unfocused, 1″, 0.5 MHz Olympus V301 sweeping from 350 kHz to 700 kHz over 90 s. A 0.5 mm Mueller needle hydrophone served as the detector, where data was acquired at 20 points inside the cavity and 27 points outside the latter half, opposite the cavity (Fig. 1b). Multiple measurements were done at constant temperature to ensure result consistency.

Intensity of sound wave inside and outside the cavity was also calculated numerically using COMSOL Multiphysics software. The Linearized Navier-Stokes model coupled to Solid Mechanics physics was employed to calculate the frequency dependence of the transmission intensity averaged over an area inside and outside the cavity. The aluminum rods in water were treated as elastic, and no-slip boundary conditions were applied at the surface of the rods. Perfectly matched layers around the aluminum-water system were introduced in the simulations to consider the absorption of reflections from outside the boundaries.

3. Results and discussions

For this work, enhanced energy trapping in the cavity is examined using three frequency dependent factors: the presence of nonreciprocity, the presence of a transmission band for the 0° (forward) direction, and the degree of energy entrapment in the cavity. Further details are given below. The frequency range of 620–628 kHz was found to contain all conditions being satisfied. These frequencies are included as insets to the larger spectra for convenience. Note that the resonant frequency of the cavity lies in the range of dozens of kHz, i.e., at least one order of magnitude lower. All the effects of acoustic transmission studied here are of nonresonant nature.

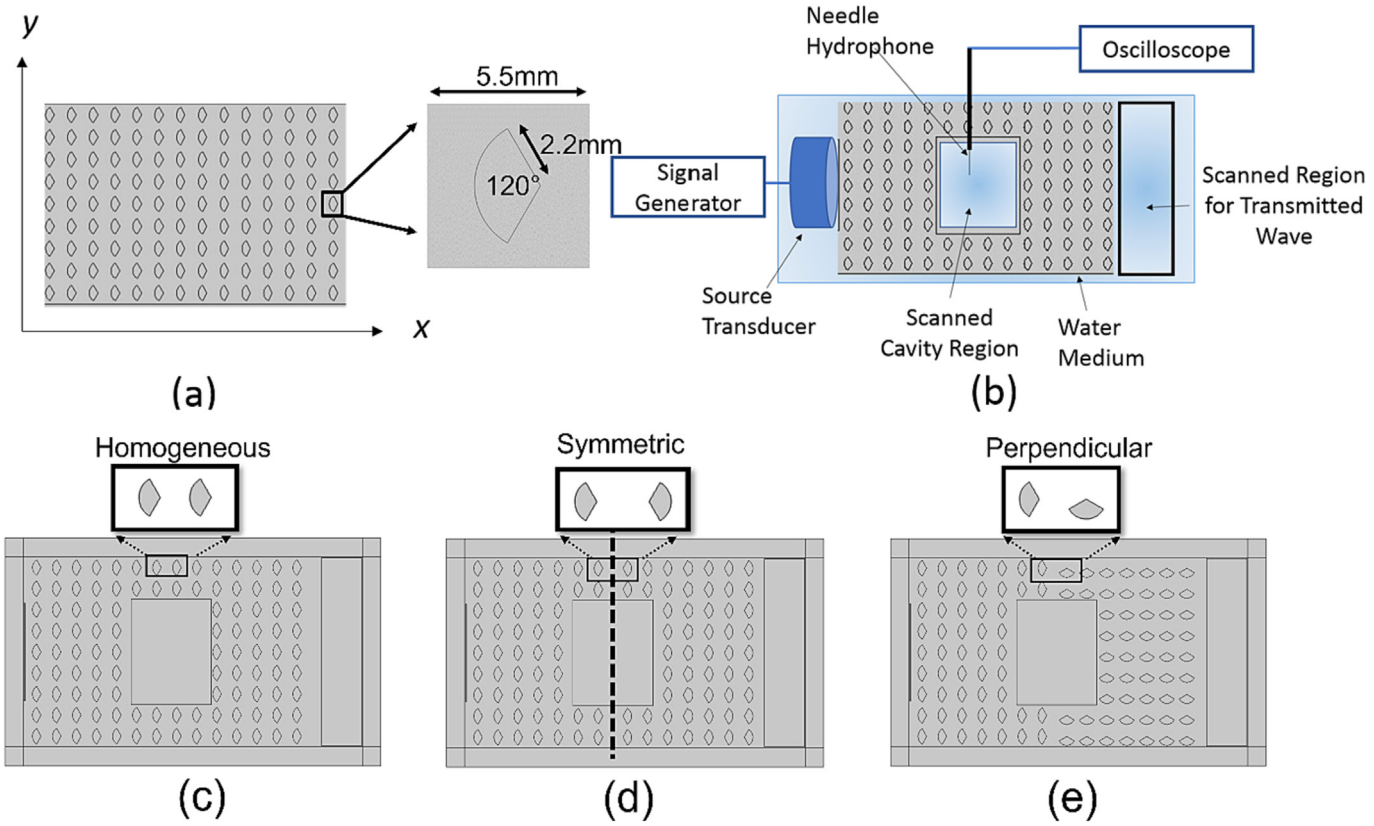

Fig. 1. Schematic representation showing (a) 14x9 aluminum rods phononic crystal along with the unit cell and, (b) experimental arrangement for measuring transmission spectra inside and outside the cavity. Image of 4x5 periods (c) cavity in a homogeneous phononic crystal, (d) symmetric cavity between two spatially inverted crystals and, (e) perpendicular cavity between two crystals rotated by 90° used in the experiments. Note that the scatterers in the incident half (left incidence) are identical for all configurations while the orientations are different for each cavity in the latter half.

Ideally, nonreciprocity is signified by the clear appearance of transmission in one direction and opaqueness in the reverse. Consider the *hypothetical* situation where for a certain frequency, the forward (0°) direction is a passing band while for reverse (180°) it is a stop band where reflection becomes strong. We use the symmetric cavity in Fig. 1d as the example illustration. Under some ideal conditions, the incident half of the crystal, oriented at 0° (forward), is transparent for incident acoustic waves, and the latter half, with orientation of the rods inverted by 180°, is reflective due to nonreciprocity. At this moment we do not discuss whether such ideal nonreciprocity is in principal possible. Here, the primary barrier is defined as the incident side of the cavity and the secondary barrier as the post cavity half of the crystal.

After traversing the cavity, the waves encounter a crystal oriented in reverse at 180°, i.e., incident on the cone of the scatterer. Reflection ensues from the secondary barrier, and the wave is sent back towards the primary barrier. However, now the primary barrier has become reflective as the incident wave is again on the 180° side of the crystal. Under these ideal conditions, the wave is allowed to enter the cavity, but it would become trapped between the reflectors due to nonreciprocity.

In a *passive and infinite* phononic crystal with lossless constituents the dispersion relation for any propagating eigenmode is real and reciprocal, i.e., $\omega(\mathbf{k}) = \omega(-\mathbf{k})$. Viscous dissipation, while breaking the hermiticity of the eigenvalue problem, does not lead to nonreciprocity in the imaginary part of eigenfrequency, even for the phononic crystals with asymmetric scatterers [24]. Thus, the proposed scenario of energy trapping cannot be realized in a passive and infinite structure since a mode with a given **k** belonging to a passing band remains a propagating mode with the same dispersion and the same decay for the reverse direction **-k**. If, however, the parameters of the crystal are time modulated, for example due to rotation of asymmetric rod, the band structure may exhibit strongly nonreciprocal bands, where a Bloch wave with wavevector **k** at frequency ω belongs to a passing band, and the wave propagating in the opposite direction fits the bandgap [26].

Here we consider only passive phononic crystals. It was discussed in Introduction that nonreciprocal transmission in passive structures appears due to broken *PT* symmetry and finite length of the crystal. The proposed scenario of energy trapping can be only partially realized since the transmission through such structure is not ideally unidirectional. The difference in forward and backward transmission has two contributions caused by asymmetry of scatterers and nonreciprocal dissipation. The larger this difference, the stronger the enhancement of energy trapping in the cavity. The asymmetric part of transmission difference cannot be measured experimentally since it is related to the transmission through a phononic crystal with inviscid background. This part can be evaluated only numerically. Truly nonreciprocal part of transmission can be obtained by subtracting the asymmetric contribution from the experimentally measured difference between forward and backward transmission. The delicate difference between asymmetry and nonreciprocity in acoustics was discussed in detail in the review [27]. Recently the nonreciprocity caused by dissipative losses was observed in acoustic transmission through lossy metasurface [28], in propagation of elastic waves [29], and light [30] in finite-size structures with broken *P* symmetry.

Asymmetry in transmission enhanced by natural nonreciprocal dissipation are the basic principles we explore for the energy trapping in this acoustic cavity. Fig. 2 contains both the experimental

and numerical results of the cavity-free lattice where we examine nonreciprocity. Measurements are shown for 590–680 kHz. Transmission for the forward and reverse directions is gathered by switching the emitter and detector without perturbing the setup. Numerical transmission for the two opposite directions was calculated by rotating the scatterers by 180°. The passing bands for the crystal are readily apparent both experimentally and numerically, with one strong transmission window and another very weak transmission window in the 590–680 kHz range (Fig. 2).

The phononic crystal samples in Fig. 1, being passive linear devices, do not possess the property of 100% unidirectional transmission. However, discrepancies between 0° and 180°, along the direction of broken mirror symmetry, are clearly seen to varying degrees in each transmission window in Fig. 2. These differences mean presence of partial unidirectionality [31] that serves as the main reason of energy trapping inside the cavity. Both factors, asymmetry and nonreciprocity contribute to the difference. Pure asymmetric contribution can be obtained only in numerical simulation with inviscid water.

Here, we focus specifically on ranges of frequencies where transmission in the forward (0°) direction is allowed, and the nonreciprocity is clearly manifested. The inset of Fig. 2a focuses on the frequency range of 620–628 kHz where transmission is apparent in the 0° direction. Similarly, the inset of Fig. 2b focuses on the same range for the numerically calculated spectra. This range demonstrates nonreciprocity-enhanced energy trapping as defined within this work and is subsequently emphasized for analysis. Discrepancies in experimental and numerical transmission spectrum arise due to a variety of factors including the complex structure and surface condition of the scatterers, condition of the medium, and slight temperature fluctuations. Nonetheless, there is good agreement between numerical and experimental observations of nonreciprocal transmission.

To evaluate nonreciprocity, we create a metric

$$\xi = \frac{|T_{180} - T_0|}{|T_{180} + T_0|} \tag{1}$$

based on measured transmissions along 0° and 180° directions, where $T_{0(180)}$ represent the linear transmission values in the 0° (180°) directions. Fig. 3a(b) shows the experimentally (numerically) measured nonreciprocity ξ in the transmission band for the 0° and 180° direction in the frequency range of interest. In the case of ideally unidirectional transmission, $\xi = 1$, which is the maximum possible value. Here, frequencies where ξ is closer to 1 indicate larger difference between 0° and 180° directions. The insets concentrate on the 620–628 kHz range where in addition to nonreciprocal transmission, energy trapping inside a cavity created in the crystal is also demonstrated (inset of Fig. 3).

To demonstrate the impact of nonreciprocity, we begin by positing sound not be generated within the cavity, but instead inserted into the cavity from outside where it is incident onto an outer boundary. In our ideal consideration of nonreciprocity as used for energy trapping, we require the primary barrier to be nonreciprocal and transparent for incident sound, the secondary barrier to be the nonreciprocal orientation of the primary barrier and nonreciprocity to contribute to reflection. Thus, incident sound propagates into the cavity, and under these circumstances, all energy entering becomes trapped due to backscattering. On the contrary, a reciprocal cavity is fed by energy through a transmitting channel. Through this channel the energy leaks to the environment.

We define the extent of energy trapping within the cavity to be quantified using a leak coefficient (τ) of the phononic crystal calculated as

$$\tau = \frac{OC}{IC} \tag{2}$$

where OC is the averaged linear intensity transmitted through the entire structure and contained in the area outside the crystal opposite the emitter and cavity (Fig. 1b, transmitted wave region), and IC is the averaged linear intensity inside the cavity (Fig. 1b, cavity region). Under ideal conditions, if all energy is trapped in the cavity, $IC \to \infty$, while $OC \to 0$, leading to lower τ indicating relatively increased trapping. While such cavity is theoretically impossible due to the limitations imposed by the second law of thermodynamics [32], it is clear that the frequencies where the values of τ are closer to 0 correspond to larger trapping of energy inside the cavity.

The average linear intensity inside and outside the homogeneous (Fig. 1c) and symmetric (Fig. 1d) cavity with the associated leak coefficients are plotted in Fig. 4 for the frequency range of 590–680 kHz. As discussed, energy trapping of sound in a cavity requires higher intensity of sound inside the cavity (IC) with low leakage outside the cavity (OC). Fig. 4a and 4d showcase the average linear intensity inside the cavities for the experiment and simulation, respectively.

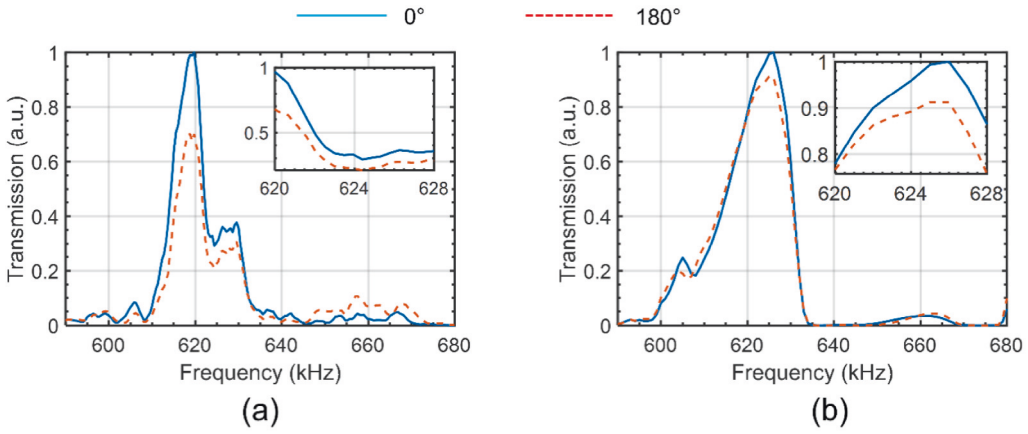

Fig. 2. (a) Experimentally measured transmission spectra for cavity free phononic crystal shown in Fig. 1c in forward direction (0°, blue curve) and reverse direction (180°, red curve). (b) Numerically calculated transmission spectra for 14X9 aluminum rods in viscous water. Inset shows magnified transmission spectra in the frequency range where the frequency dependent metric for nonreciprocity enhanced energy trapping are met. (For interpretation of the references to colour in this figure legend, the reader is referred to the web version of this article.)

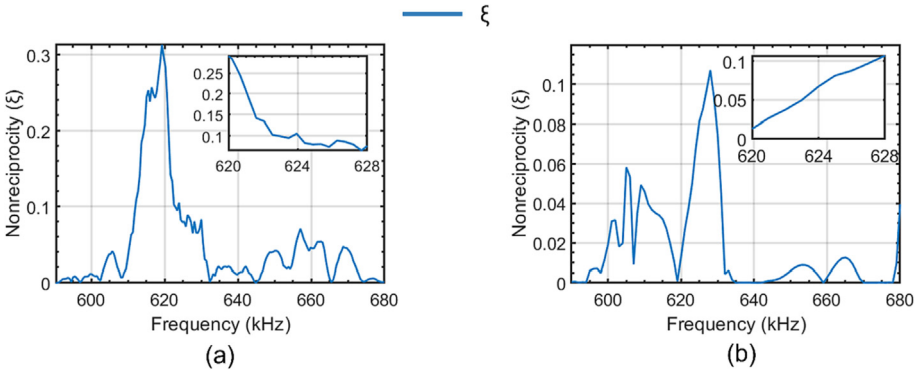

Fig. 3. (a) Nonreciprocity (ξ) in experimental transmission spectra defined by Eq. (1). (b) Nonreciprocity (ξ) associated with numerically calculated transmission spectra. Inset focusses on the frequency range where energy trapping conditions are met for experiment and simulations.

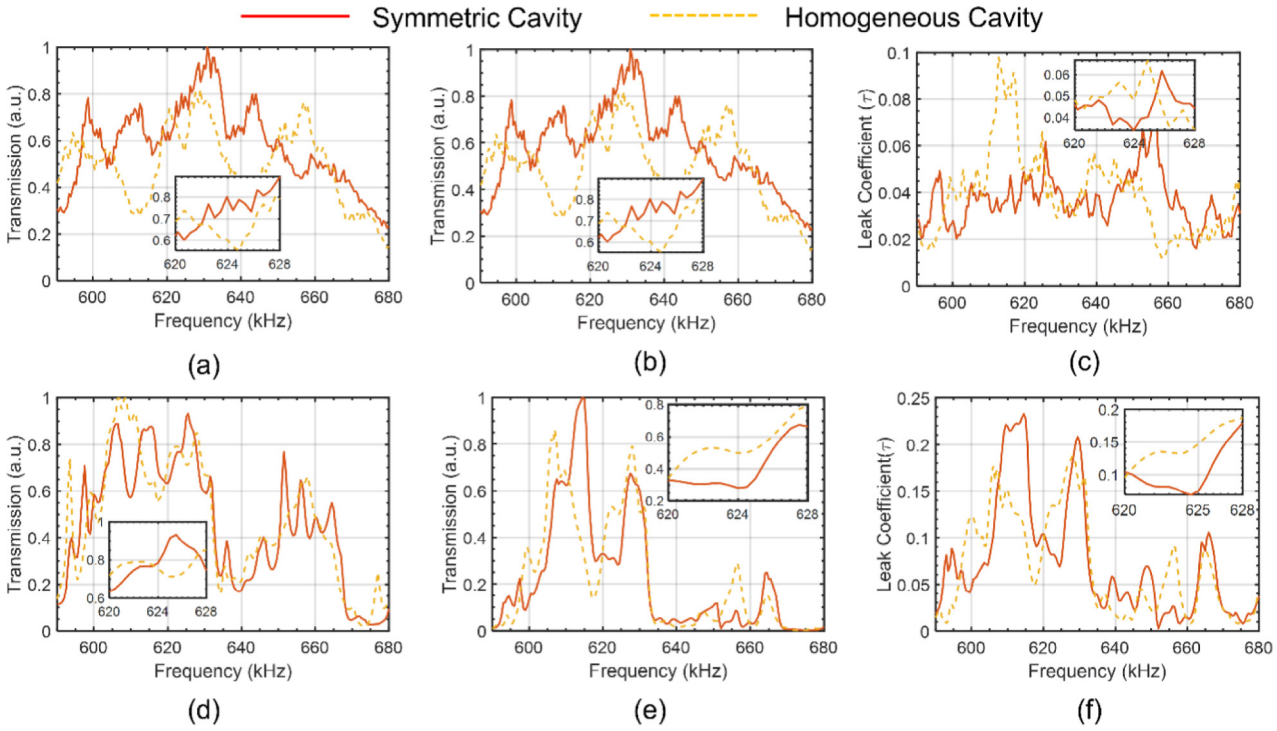

Fig. 4. Experimentally measured transmission spectra for homogeneous cavity and symmetric cavity: (a) inside the cavity, (b) outside the cavity and corresponding (c) leak coefficient τ calculated from Eq. (2). Numerically calculated transmission spectra: (d) inside the cavity, (e) outside the cavity, and corresponding (f) leak coefficient τ.

Both the homogeneous (Fig. 1c) and symmetric (Fig. 1d) arrangements have higher sound intensity inside the cavity at various frequency ranges as compared to each other. However, to show the trapping of energy due to the nonreciprocity, frequencies are selected at which, in addition to higher intensity inside the cavity, the minimum leakage of energy outside the cavity is also demonstrated for the symmetric arrangement. Fig. 4b and 4e show the intensity measured outside the cavity for experiment and simulations. The leak coefficient, τ, calculated by Eq. (2), is plotted in Fig. 4c and 4f. The experimentally measured frequency range of 620–628 kHz (inset of Fig. 3a-c) shows higher intensity of sound inside the homogeneous cavity and lower intensity outside the cavity, thus having lower leak coefficient τ (Fig. 4a-c). Maximum difference in τ between the symmetric cavity and homogeneous cavity is observed at 624 kHz with τ = 0.03 for symmetric cavity showing very low leakage of energy outside the cavity and enhanced energy trapping inside the cavity. Similarly, the same frequency range of 620–628 kHz (inset of Fig. 4d-f) shows enhanced energy trapping obtained numerically with lowest $\tau = 0.06$ at 624 kHz.

As described prior, the three frequency dependent metrics of the presence of a transmission band for the 0° direction (Fig. 2), the presence of nonreciprocity (Fig. 3), and the degree of energy entrapment in the cavity (Fig. 4) are fulfilled experimentally and numerically for the frequency range of 620–628 kHz, all together demonstrating the nonreciprocity derived energy trapping in the symmetric cavity.

Although, the symmetric cavity utilizes nonreciprocity by having two opposing orientations of asymmetric scatterers on each side of the cavity, the homogeneous cavity also has an asymmetric orientation of the scatterers along the direction of propagation. To study the effect of having symmetric orientation of the scatterers along the direction of propagation as the secondary barrier, a perpendicular cavity is constructed by rotating the scatterers in the

secondary barrier along the y-axis (Fig. 1e). Experimentally measured and numerically calculated intensity of sound wave inside and outside the perpendicular cavity compared to the symmetric arrangement is plotted in Fig. 5. The perpendicular cavity maintains lower average intensity inside the cavity and higher average intensity outside the cavity at frequency ranges of 620–628 kHz, leading to a higher leak coefficient τ. Higher leak coefficient indicates that the secondary barrier has also become more transparent to the incident waves, thus allowing increased energy to escape the crystal through transmission. Consequently, changing the orientation of the scatterers in the latter half of the cavity can result in "dumping" of the stored energy making the cavity tunable for various applications in which delay of sound waves in time are required.

The simulated acoustic pressure maps at 624 kHz for the three cavities are shown in Fig. 6. These results visually demonstrate the primary barrier of the cavity allowing the acoustic waves to pass. This agrees with the transmission spectra, as this frequency lies in the passing band of the phononic crystal at 0°. The impact of the orientation of the secondary cavity barrier is also visually apparent in Fig. 6. The symmetric cavity with the secondary barrier oriented at 180° shows reflection of the post-primary transient wave supported by the presence of nonreciprocal effects in the transmission band (Fig. 6b). Comparatively, though backscattering is observable in all orientations, both the homogeneous and perpendicular cavity show increased wave penetration through the secondary barrier. These results show consistency with all the above observations of nonreciprocity enhanced energy trapping in the symmetric cavity.

Discrepancies in experimental and numerical results are due to the complex structure of the scatterers along with the surface roughness of the scatterers in the experiments. If the height of surface roughness is comparable or exceeds the thickness of the boundary layer δ, the dynamics of the vorticity mode is strongly affected. Also, the area of the fluid–solid boundary increases. Both these factors lead to increase of the dissipative losses and nonreciprocity. Enhancement of nonreciprocity in transmission caused by surface roughness was first mentioned in Ref. [20].

It is worthwhile to compare the contribution of surface roughness in enhancement of energy trapping for the present system. Whereas the contributions of nonreciprocity can be distinguished numerically, it is impossible to completely decouple contributions of asymmetry and nonreciprocity experimentally due to surface features. Ref. [24] investigates the contribution to nonreciprocity of surface features in a complete cylinder with one half of the surface flat and the other half rough. It was shown that increases in surface roughness increased the local dissipation and the nonreciprocity. Consequently, wave transmission was numerically calculated for the asymmetric scatterers with and without surface roughness for the present system. Surface roughness was introduced numerically by constructing square wells on the surface of the scatterers. The size of the surface roughness was 50 μm which was 10 times greater than the size of the viscous layer. Nonreciprocity contribution (α) to the transmission through periodic finite-length crystal (without cavity) in the frequency range of 620–628 kHz is calculated using the following metric:

$$\alpha = \frac{\xi(R) - \xi(0)}{\xi(0)} \tag{3}$$

where $\xi(0)$ is the nonreciprocity for system of scatterers without surface roughness and $\xi(R)$ is the nonreciprocity with surface roughness. We use roughness to approximate the contributions of viscosity to increased dissipation in accordance with [24]. From the definition of α in Eq. (3), it can be deduced that larger α implies larger nonreciprocal contribution in the wave transmission. Fig. 7a shows the behavior of α with respect to frequency. It is clearly seen from the figure that at select frequencies, surface roughness contribution to nonreciprocity is more than 5 times than that of scatterers without surface roughness with an increase of 2.5 times for 624 kHz.

To further evaluate the effect of surface roughness induced nonreciprocity on the leak coefficient of the cavity, a metric β is created which is defined by:

$$\beta = \left[\frac{\tau(0) - \tau(R)}{\tau(0)}\right] \tag{4}$$

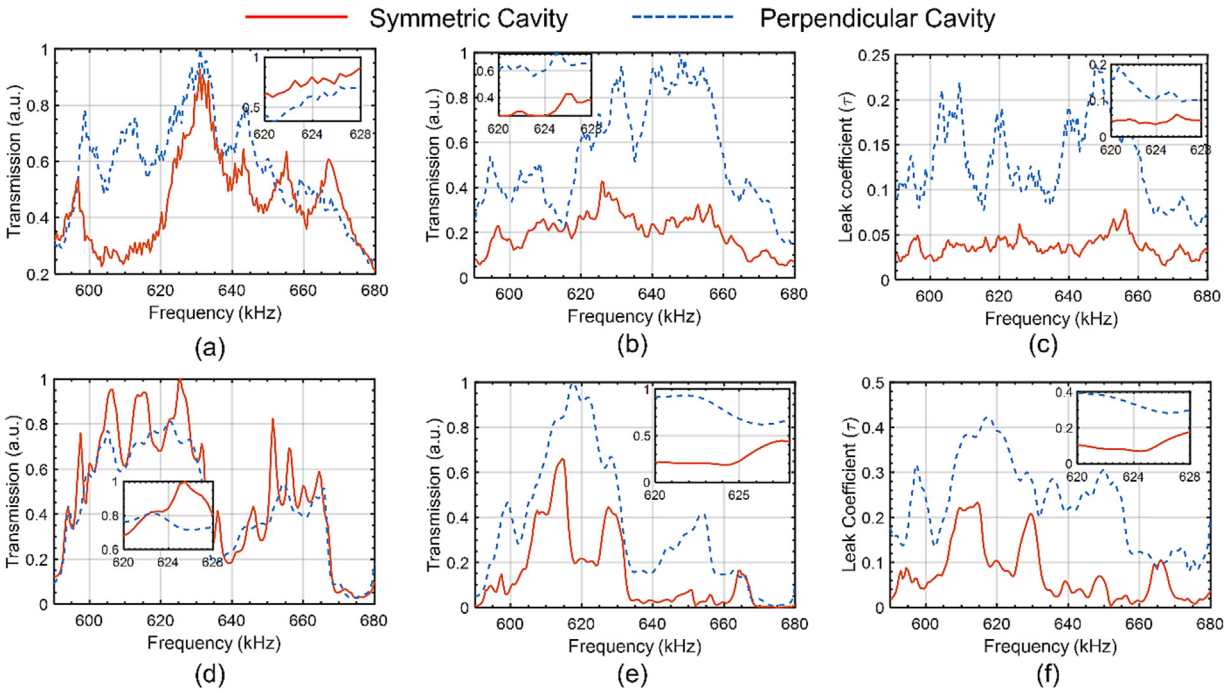

Fig. 5. Experimentally measured transmission spectra for perpendicular cavity and symmetric cavity: (a) inside the cavity, (b) outside the cavity and corresponding (c) Leak Coefficient τ calculated from Eq. (2). Numerically calculated transmission spectra: (d) inside the cavity, (e) outside the cavity, and corresponding (f) leak coefficient τ.

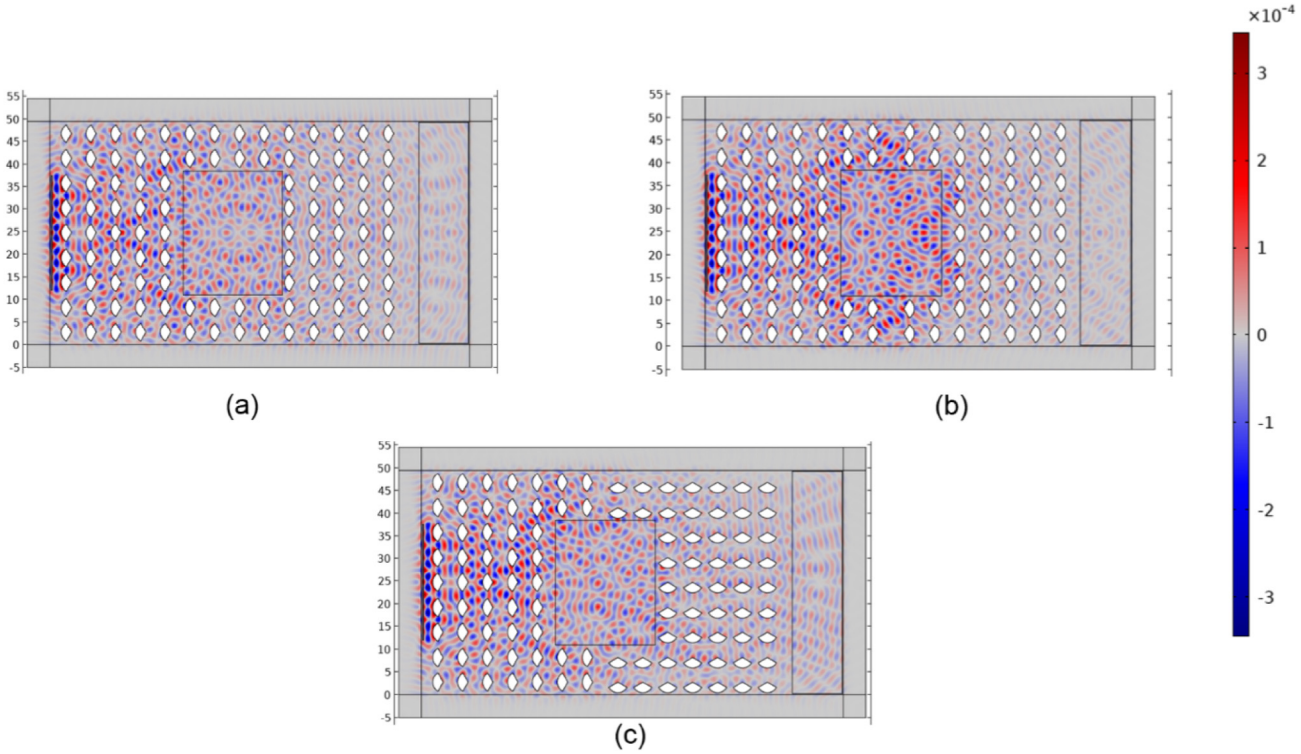

Fig. 6. Computationally simulated acoustic pressure map at 624 kHz for: (a) homogeneous cavity, (b) symmetric cavity, and (c) perpendicular cavity. Note strong reflection at the right boundary of the symmetric cavity.

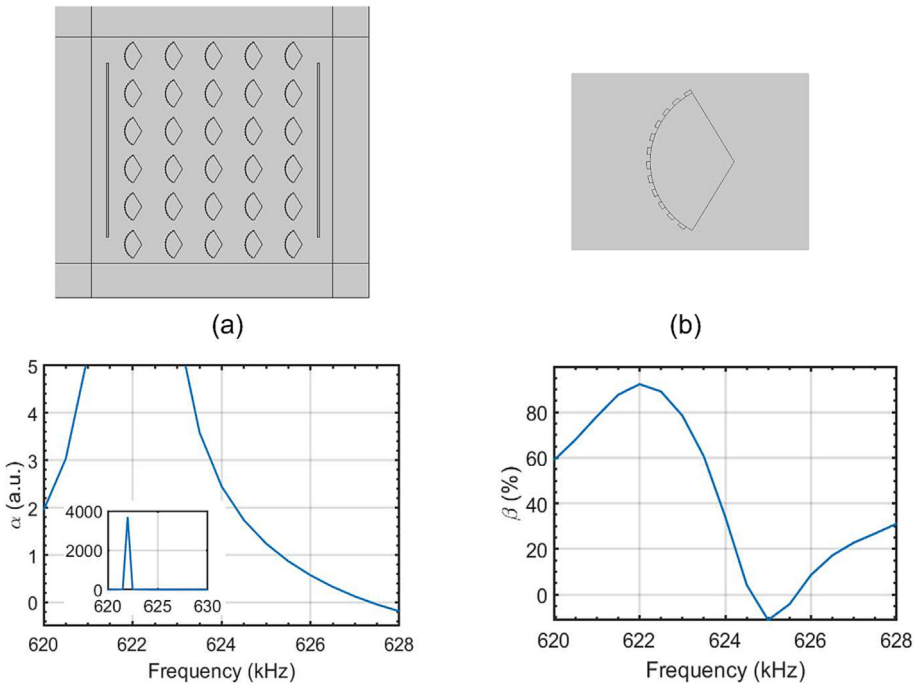

Fig. 7. (a) Phononic crystal with rough scatterers. (b) unit cell of the crystal. Contribution of surface roughness in nonreciprocity in (c) transmission (Eq. (3)) through periodic crystal shown in Fig. 1c with rough and smooth scatterers and in (d) leak coefficient improvement Eq. (4) in symmetric cavity.

where $\tau(R)$ is the leak coefficient of the cavity with scatterers having surface roughness and $\tau(0)$ is leak coefficient when the scatterers surface is smooth. From Eq. (4), greater β means lower leak coefficient for the rough scatterers case, and correspondingly better trapping. The values of β for the frequency range of 620–628 kHz is depicted in Fig. 7b. Improvement in leak coefficient up to 92% is observed in the given frequency range and 34% improvement is observed at 624 kHz. The results in Fig. 7 collectively support that presence of roughness on the surface of the scatterers indeed induces nonreciprocity that enhances the energy trapping.

4. Conclusions

Nonreciprocity in transmission through a phononic crystal with asymmetric scatterers and naturally viscous background is utilized to enhance energy trapping in a cavity formed inside the crystal. It is established, comparing cavities of different symmetry, that the optimized trapping occurs for a symmetric cavity between two twinned crystals. For this geometry, the incoming beam freely penetrates inside the cavity and due to partial unidirectionality more energy remains inside than radiates outside at each reflection from its boundaries. Though unidirectionality is only partial with transparency in one direction and opaqueness in the reverse, the differences in transmission due to nonreciprocity results in additional reflection from the secondary boundary in the symmetric cavity. Subsequently, the backscattering from primary and secondary barriers result in enhanced energy trapping as confirmed both numerically and experimentally. Furthermore, a tunable cavity can be made to trap energy (symmetric cavity) in one orientation of the asymmetric scatterers and dump in another orientation of the asymmetric scatterers (perpendicular cavity). Improvements for efficient energy trapping through quantification of the effective cavity length with nonreciprocal, periodic barriers provide an opportunity for rich theoretical, numerical, and experimental investigation.

Data availability

Data will be made available on request.

Declaration of Competing Interest

The authors declare that they have no known competing financial interests or personal relationships that could have appeared to influence the work reported in this paper.

Acknowledgement

This work is supported by an Emerging Frontiers in Research and Innovation grant from the U.S. National Science Foundation (Grant No. 1741677).

References

[1] Sigalas M, Economou EN. Band structure of elastic waves in two dimensional systems. Solid State Commun 1993;86(3):141–3.
[2] Kushwaha MS, Halevi P, Dobrzynski L, Djafari-Rouhani B. Acoustic band structure of periodic elastic composites. Phys Rev Lett 1993;71(13):2022–5.
[3] Vasseur JO, Djafari-Rouhani B, Dobrzynski L, Kushwaha MS, Halevi P. Complete acoustic band gaps in periodic fibre reinforced composite materials: the carbon/epoxy composite and some metallic systems. J Phys Condens Matter 1994;6(42):8759–70.
[4] Li YF, Meng F, Zhou S, Lu M-H, Huang X. Broadband All-angle Negative Refraction by Optimized Phononic Crystals. Sci Rep 2017;7:7445.
[5] Yang S, Page JH, Liu Z, Cowan M, Chan CT, Sheng P. Focusing of sound in a 3D phononic crystal. Phys Rev Lett 2004;93:024301.
[6] Flores J, Gutiérrez L, Méndez-Sánchez RA, Monsivais G, Mora P, Morales A. Anderson localization in finite disordered vibrating rods. Europhys Lett 2013;101(29):67002.
[7] Graham IS, Piché L, Grant M. Experimental evidence for localization of acoustic waves in three dimensions. Phys Rev Lett 1990;64(26):3135–8.
[8] Hu H, Strybulevych A, Page JH, Skipetrov SE, van Tiggelen BA. Localization of ultrasound in a three-dimensional elastic network. Nat Phys 2008;4(12):945–8.
[9] Dhillon J, Bozhko A, Walker E, Neogi A, Krokhin A. Localization of ultrasound in 2D phononic crystal with randomly oriented asymmetric scatterers. J Appl Phys 2021;129:134701.
[10] Khelif A, Choujaa A, Djafari-Rouhani B, Wilm M, Ballandras S, Laude V. Trapping and guiding of acoustic waves by defect modes in a full-band-gap ultrasonic crystal. Phys Rev B - Condensed Matter Mater Phys 2003;68(21):214301.
[11] Li F, Liu J, Wu Y. The investigation of point defect modes of phononic crystal for high Q resonance. J Appl Phys 2011;109(12):124907.
[12] Wu F, Hou Z, Liu Z, Liu Y. Point defect states in two-dimensional phononic crystals. Phys Lett, Sect A: Gen, Atomic Solid State Phys 2001;292(3):198–202.
[13] Kafesaki M, Sigalas MM, García N. Frequency modulation in the transmittivity of wave guides in elastic-wave band-gap materials. Phys Rev Lett 2000;85(19):4044–7.
[14] Khelif A, Djafari-Rouhani B, Vasseur JO, Deymier PA, Lambin P, Dobrzynski L. Transmittivity through straight and stublike waveguides in a two-dimensional phononic crystal. Phys Rev B - Condensed Matter Mater Phys 2002;65(17):174308.
[15] Sigalas MM, Biswas R, Ho KM, Soukoulis CM, Crouch DD. Waveguides in three-dimensional metallic photonic band-gap materials. Phys Rev B - Condensed Matter Mater Phys 1999;60(7):4426–9.
[16] Colombi A, Roux P, Rupin M. Sub-wavelength energy trapping of elastic waves in a metamaterial. J Acoust Soc Am 2014;136(2):EL192–8.
[17] Khelif A, Djafari-Rouhani B, Vasseur O, Deymier A. Transmission and dispersion relations of perfect and defect-containing waveguide structures in phononic band gap materials. Phys Rev B - Condensed Matter Mater Phys 2003;68(2):024302.
[18] Ziaei-Moayyed M, Su MF, Reinke C, El-Kady IF, Olsson RH. Silicon carbide phononic crystal cavities for micromechanical resonators. Proceedings of the IEEE International Conference on Micro Electro Mechanical Systems (MEMS), Cancun, Mexico, 2011.
[19] Wu LY, Chen LW, Liu CM. Acoustic energy harvesting using resonant cavity of a sonic crystal. Appl Phys Lett 2009;95(1):013506.
[20] Walker E, Neogi A, Bozhko A, Zubov Y, Arriaga J, Heo H, et al. Nonreciprocal linear transmission of sound in a viscous environment with broken P symmetry. Phys Rev Lett 2018;120(20):204501.
[21] Rayleigh JWS. Theory Sound, Vol. I. NY: Dover; 1945.
[22] Fleury R, Sounas D, Haberman MR, Alù A. Nonreciprocal Acoustics. Acoust Today 2015;11:14–21.
[23] Caloz C, Alù A, Tretyakov S, Sounas D, Achouri K, Deck-Léger Z-L. Electromagnetic nonreciprocity. Phys Rev Appl 2018;10:047001.
[24] Heo H, Walker E, Zubov Y, Shymkiv D, Wages D, Krokhin A, et al. Nonreciprocal acoustics in viscous environment. Proc R Soc A 2020;476:20200657.
[25] Ibarias M, Zubov Y, Arriaga J, Krokhin AA. Phononic crystal as a homogeneous viscous metamaterial. Phys Rev Res 2020;2:022053(R).
[26] Nassar H, Chen H, Norris A, Huang GL. Quantization of band tilting in modulated phononic crystals. Phys Rev B 2018;97:014305.
[27] Maznev AA, Every AG, Wright OB. Reciprocity in reflection and transmission: what is a 'phonon diode'? Wave Motion 2013;50(4):776–84.
[28] Li Y, Shen C, Xie Y, Li J, Wang W, Cummer SA, et al. Tunable asymmetric transmission via lossy acoustic metasurfaces. Phys Rev Lett 2017;119:035501.
[29] Tanaka Y, Shimomura Y, Nishiguchi N. Acoustic wave rectification in viscoelastic materials. Jpn J Appl Phys 2018;57:034101.
[30] Huang X, Lu C, Liang C, Tao H, Liu Y-C. Loss-induced nonreciprocity. Light Sci Appl 2021;10:30.
[31] Serebryannikov AE, Ozbay E. Unidirectional transmission in non-symmetric gratings containing metallic layers. Opt Express 2009;17:13335–45.
[32] Mann SA, Sounas DL, Alù A. Nonreciprocal cavities and the time–bandwidth limit. Optica 2019;6(1):104.